

**Supplemental Figure 1: Table of transcription factors analyzed in TF-seq experiment**

**Supplemental Figure 2: Analysis of ChIP-Seq dataset reveals binding of BMAL1 to an E-box in the *Nrf2* promoter**

Fastq data for ChIP-seq samples from GEO series GSE95712 were analyzed using Genome wide Event finding and Motif discovery (GEM) and visualized with UCSC genome browser. A significant peak (p-value = 0.0032, q-value = 0.0059) was discovered overlapping the E-box site in the *Nrf2* promoter, highlighted by blue line, in basal peritoneal macrophages.

**Supplemental Figure 3: NRF2 is under regulation of BMAL1**

(A) Peritoneal cells were isolated from wild type mice at 4 hr intervals (ZT0, ZT4, ZT8, ZT12, ZT16 and ZT20) and *Bmal1* mRNA was measured by qPCR. A cosinor regression model was used to test the null hypothesis that the amplitude of expression = 0. The presence of the red line indicates the presence of a significant rhythm (n= 3-6). (B) *Bmal1*<sup>+/+</sup> and *Bmal1*<sup>-/-</sup> BMDMs were synchronized using 50 % horse serum. RNA was extracted at 4 hr intervals for 36 hr and *Bmal1* mRNA was measured by qPCR. A cosinor regression model was used to test the null hypothesis that the amplitude of expression = 0. The presence of the red line indicates the presence of a significant rhythm (n=3). (C) Wild type C57Bl6 mice were injected with PBS or 5 mg/kg LPS for 90 minutes before harvesting peritoneal cells and lysing in lysis buffer. BMAL1 and NRF2 levels were measured by western blotting. (D) *Nrf2* mRNA was measured by qPCR in wild type

BMDMs transfected with scrambled siRNA or siRNA targeting *Bmal1* following 24 hr of LPS (100 ng/mL) (n=6). (E) Immunoblot of NRF2 levels following 24 hr of LPS (100 ng/mL) in wild type BMDMs transfected with scrambled siRNA or siRNA targeting *Bmal1*. Immunoblots shown are a representative of at least three independent experiments. Values provided below each lane indicate relative densitometry of each band. Graphs (A-B) statistical significance was determined by establishing a cosinor regression model. Statistical significance of (D) was determined by one-way ANOVA.  $**P \leq 0.01$ .

#### **Supplemental Figure 4: Efficiency of knockdown experiments**

BMDMs were transfected with scrambled siRNA or siRNA targeting (A) *Bmal1*, (B) *Nrf2*, or (C) *Keap1* and mRNA was measured by qPCR as a marker of knockdown efficiency. Statistics were generated by unpaired Student's t test (n=3).  $***P \leq 0.001$ .

#### **Supplemental Figure 5: NRF2 antioxidant targets are decreased with *Bmal1* deletion or knockdown**

(A) *Hmox1* and (B) *Gsr* mRNA was measured by qPCR in *Bmal1*<sup>+/+</sup> and *Bmal1*<sup>-/-</sup> BMDMs following 4 hr of hydrogen peroxide stimulation (50  $\mu$ M) (n=3). (C) *Hmox1*, (D) *Gsr*, and (E) *Nqo1* mRNA was measured by qPCR in wild type BMDMs transfected with scrambled siRNA or siRNA targeting *Bmal1* following 24 hr of LPS stimulation (100 ng/ml) (n=4-6). Statistics were generated by one-way ANOVA  $*P \leq 0.05$ ,  $**P \leq 0.01$ , and  $***P \leq 0.001$ .

**Supplemental Figure 6: Full list of genes and fold change at ZT12 relative to ZT0 analyzed in oxidative stress analysis array**

**Supplemental Figure 7: Increased ROS production with *Bmall* knockdown**

Wild type BMDMs were transfected with a scrambled siRNA or siRNA targeting *Bmall*. The cells were treated with LPS (100 ng/mL) for 24 hr followed by CellROX staining. ROS was then measured via flow cytometry (n=5).

**Supplemental Figure 8: Increased inflammation with *Bmall* deletion or knockdown**

Peritoneal cells were isolated from *Bmall*<sup>+/+</sup> and *Bmall*<sup>-/-</sup> mice and treated with LPS (100 ng/mL) for 24 hr *ex vivo*. Pro-IL-1 $\beta$  was detected by western blotting. (B, C) *Bmall*<sup>+/+</sup> and *Bmall*<sup>-/-</sup> BMDMs were treated with LPS (100 ng/mL) for 24 hr before measuring (B) IL-6 and (C) TNF $\alpha$  by ELISA (n=4). (D, E) Wild type BMDMs were transfected with scrambled siRNA or siRNA targeting *Bmall* and treated with LPS (100 ng/mL) for 24 hr and (D) *Il1b* mRNA was measured by qPCR (n=6) and (E) pro-IL-1 $\beta$  was measured by immunoblot. Immunoblots shown are a representative of at least three independent experiments. Values provided below each lane indicate relative densitometry of each band. Statistical significance of (A, B, C, D), was generated by one-way ANOVA \* $P \leq 0.05$  and \*\*\* $P \leq 0.001$ .

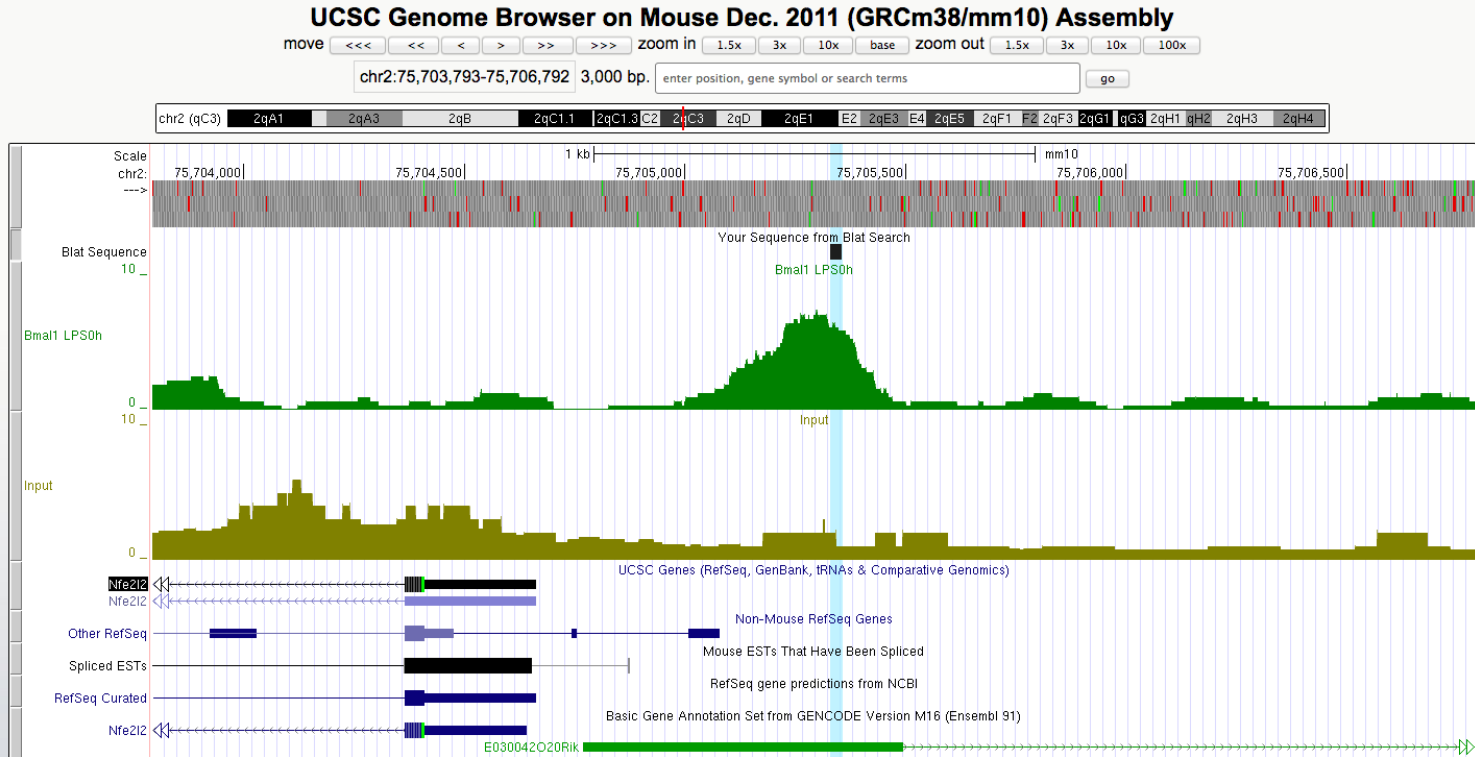
**Supplemental Figure 9: *Keap1* knockdown or DEM treatment boosts expression of *Nqo1* in *Bmall*<sup>-/-</sup> macrophages**

*Bmal1*<sup>+/+</sup> and *Bmal1*<sup>-/-</sup> BMDMs were transfected with scrambled siRNA or siRNA targeting *Keap1* and treated with LPS (100 ng/mL). (A) *Nqo1* mRNA was measured by qPCR (n=4). (B) *Bmal1*<sup>+/+</sup> and *Bmal1*<sup>-/-</sup> BMDMs were pre-treated with either 100  $\mu$ M DEM or 10 mM NAC before LPS (100 ng/mL) stimulation. *Nqo1* mRNA was measured by qPCR (n=3). Statistical significance of all graphs was determined by one-way ANOVA \*\* $P \leq 0.01$ , and \*\*\* $P \leq 0.001$ .

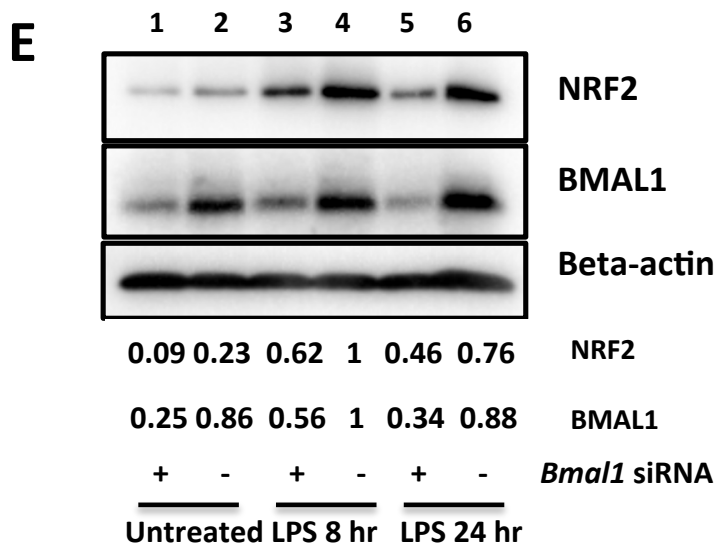
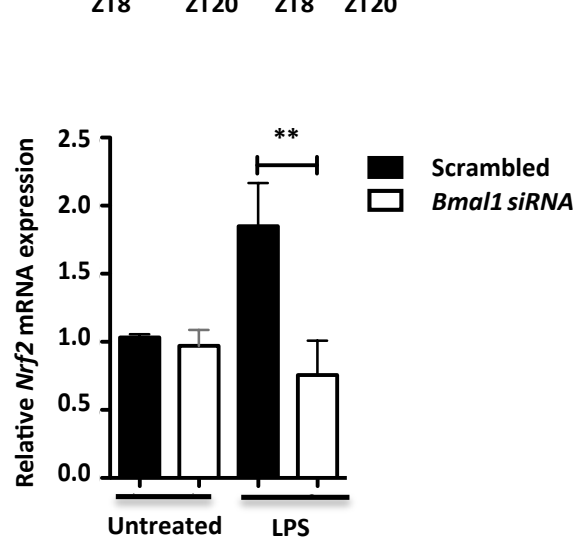
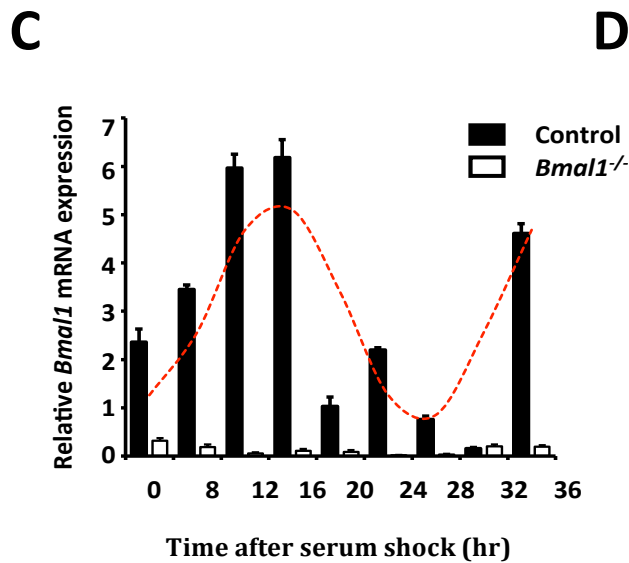
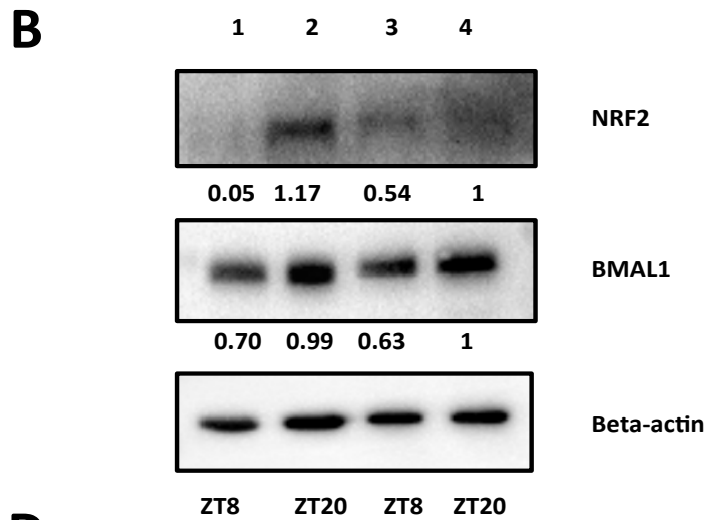
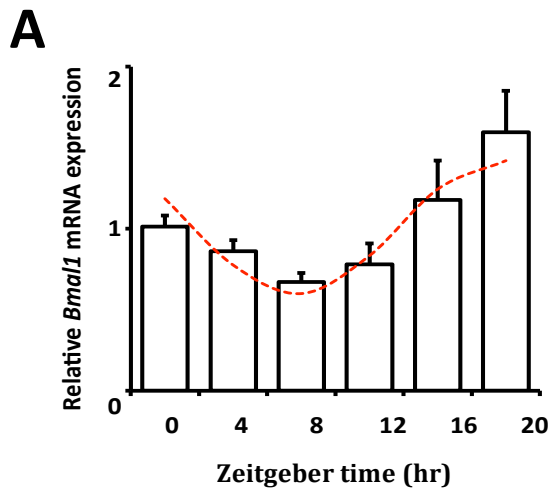
# Supplemental Figure 1

Pathway	Transcription Factors
Aryl hydrocarbon receptor (AHR)	AHR
Amino acid deprivation (AARE)	ATF4
AP-1 (MAPK)	FOS, JUN
Apoptosis	TRP53
Antioxidant response element (ARE)	NFE2L2 (NRF2)
c-MAF	MAF
C-REL (alternative NF-κB)	REL
C/EBPα	CEBPA
C/EBPβ	CEBPB
Circadian cycle	CLOCK
Constitutive enhancer	NFYA
Constitutive enhancer	SP1
Cyclic AMP	CREB1
Early growth response	EGR1
ER stress element (ERSE)	XBP1
Farnesoid X receptor	NR1H4 (FXR)
GATA3	GATA3
Glucocorticoid receptor	NR3C1 (GR)
Hedgehog	GLI1
Hepatocyte nuclear factor 4	HNF4a
Hippo	TEAD1
Hypoxia	HIF1A
IFNβ	AP-1, IRF3, IRF7, NF-κB
Insulin (PI3K/AKT)	FOXO1
IRF1	IRF1
IRF3	IRF3
IRF3/IRF7	IRF3, IRF7
Liver X receptor	NR1H3 (LXR)
Lysosomal biogenesis	TFEB
MAPK	ELK1
NF-κB	NFKB1, RELA (p50, p65)
Notch	NICD, CBF1 (CSL, RBPJ)
PKC/Ca <sup>2+</sup>	NFATC1
PPARg	PPARg, RXRA
RELB (alternative NF-κB)	RELB
Retinoic acid (RARE)	RARA
Retinoid-related orphan receptors (RORs)	RORC
RUNX	RUNX1
Serum response element	SRF
Sis-inducible element (SIE)	STAT3
STAT4	STAT4
STAT5	STAT5a, STAT5b
STAT6	STAT6
Sterol	SREBF1
TGF-β	SMAD2, SMAD3, SMAD4
Type I IFN	STAT1, STAT2
Type II IFN	STAT1, STAT1
Unfolded protein response element (UPRE)	ATF6
Vitamin D	VDR
Wnt	LEF1, TCF7, TCF7L1, TCF7L2
Minimal promoter only	single TATA promega pGL4 series

# Supplemental Figure 2

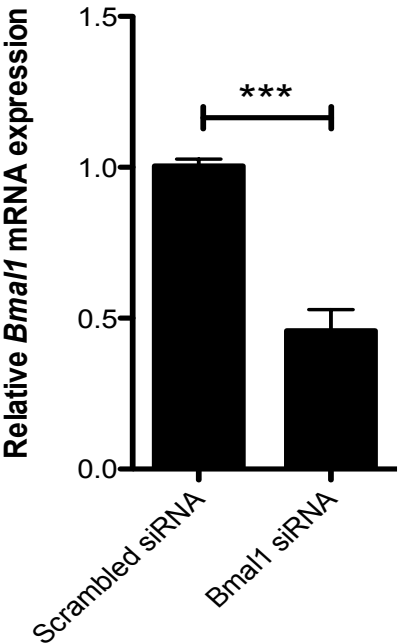


# Supplemental Figure 3

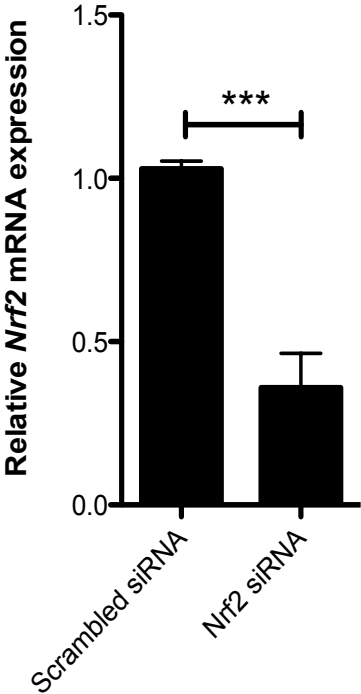


# Supplemental Figure 4

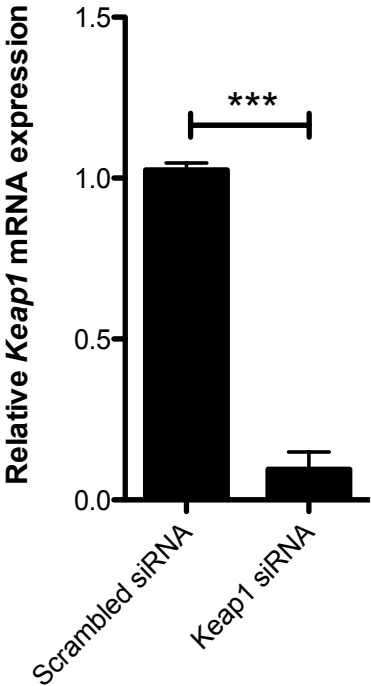
**A**



**B**



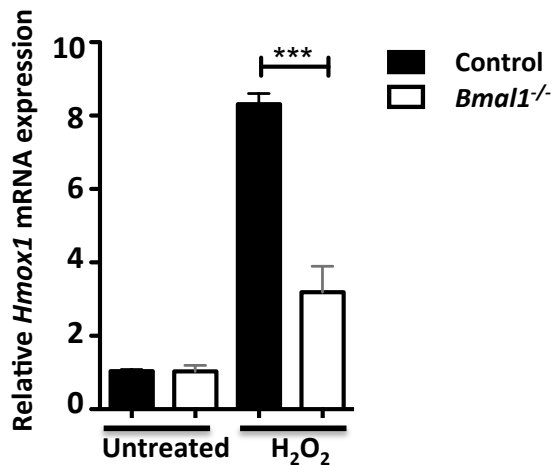
**C**



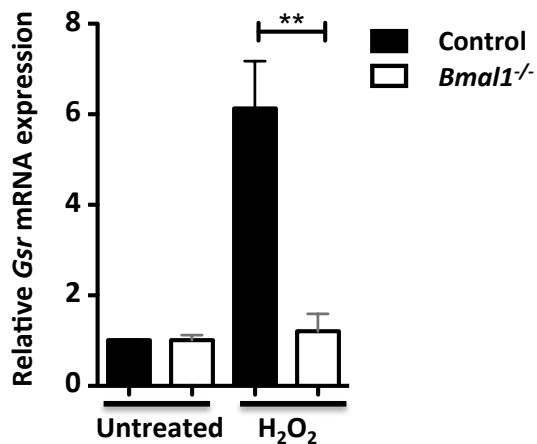


## Supplemental Figure 5

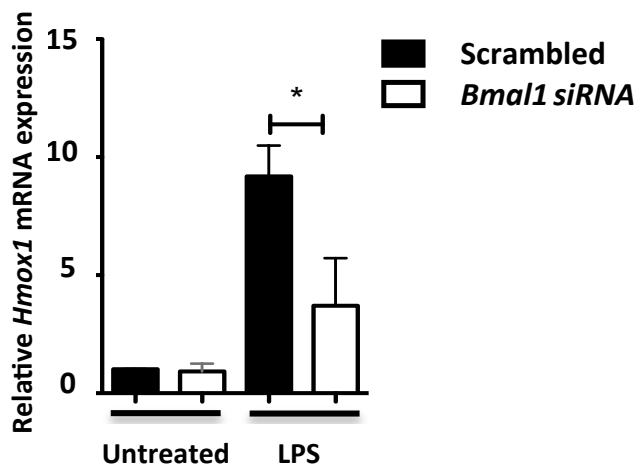
**A**



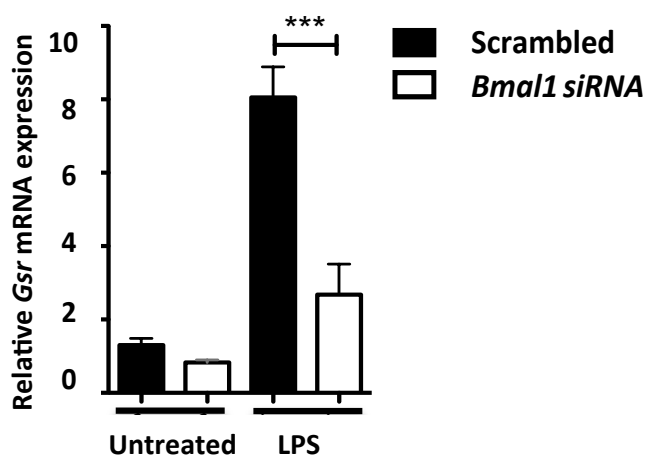
**B**



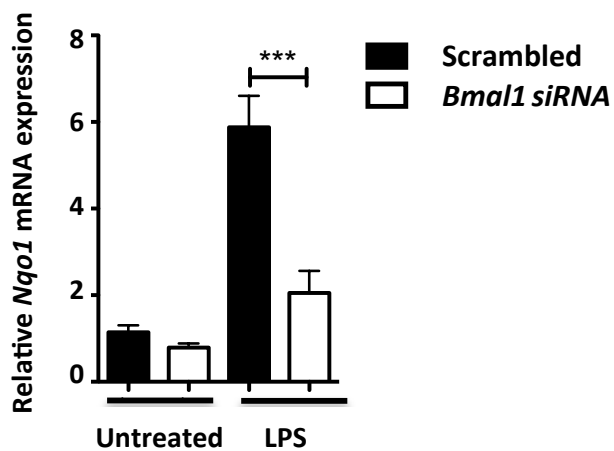
**C**



**D**



**E**



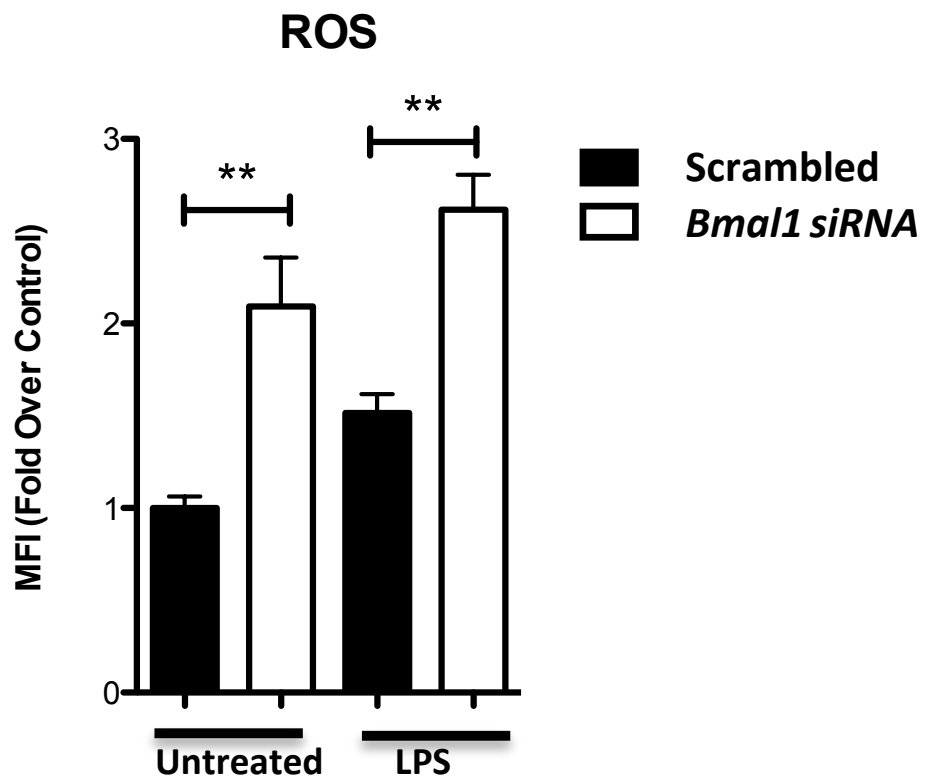
## Supplemental Figure 6

Gene	Log2-ratio
Alb	7.56
Als2	1.15
AOX1	7.72
Apc	0.79
Apoe	-0.05
Atr	1.66
Cat	0.00
CCL5	2.83
Ccs	0.76
Ctsb	-0.22
Cyba	-0.21
Cygb	7.78
Dnm2	0.19
DUOX1	8.23
Ehd2	1.56
Epx	6.83
Ercc2	1.04
Ercc6	1.76
Fancc	1.59
Fmo2	7.94
Fth1	-0.32
Gclc	0.39
Gclm	0.31
Gpx1	-0.79
Gpx2	7.74
Gpx3	0.58
Gpx4	-0.18
Gpx5	3.69
Gpx6	7.34
Gpx7	1.23
Gsr	-0.38

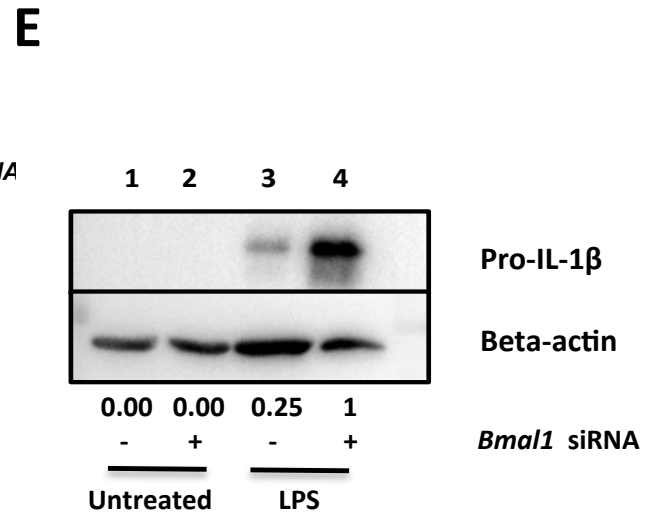
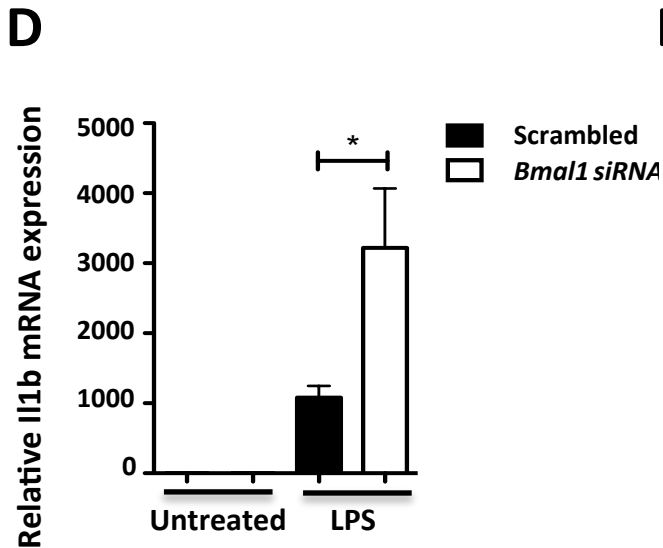
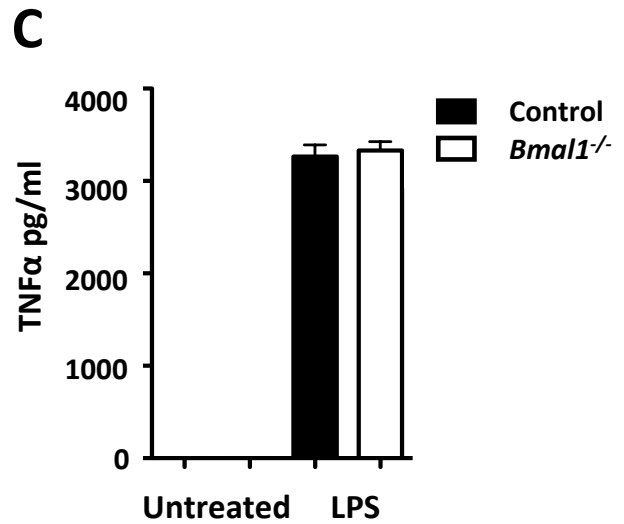
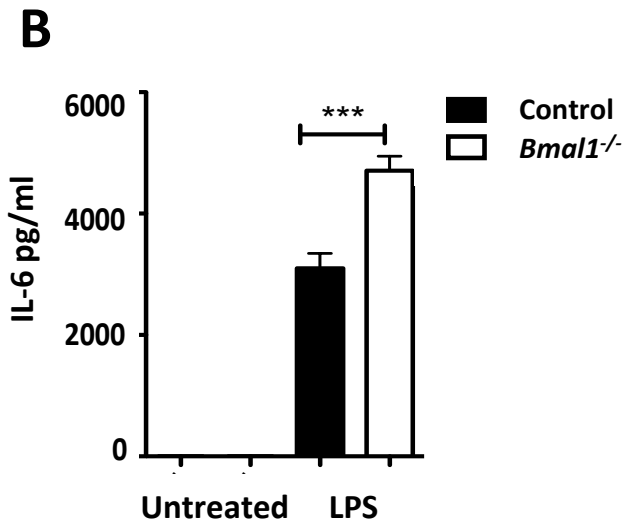
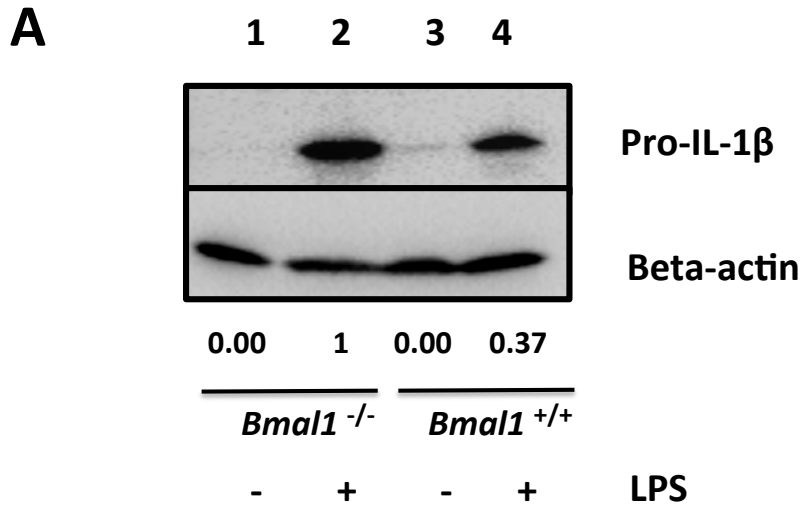
Gene	Log2-ratio
Gss	1.22
Gstk1	0.38
Gstp1	-0.33
Hmox1	-0.43
Hspa1a	-0.77
Idh1	0.15
Ift172	1.01
Il19	8.50
IL-22	8.72
Krt1	7.74
Lpo	7.40
Mb	8.18
Mpo	6.05
Ncf1	0.09
Ncf2	-0.19
Ngb	5.13
NOS2	7.59
NOX1	6.59
NOX4	6.99
Noxa1	6.26
Noxo1	3.68
Nqo1	5.07
Park7	0.01
PRDX1	1.31
Prdx2	-0.38
Prdx3	-0.06
Prdx4	-0.10
Prdx5	-0.25
Prdx6	0.05
Prnp	3.27
Psmb5	0.04

Gene	Log2-ratio
Ptgs1	0.25
Ptgs2	2.78
Rag2	7.57
Recql4	3.53
Scd1	2.19
Serpinb1b	0.45
Slc38a1	0.27
Sod1	0.69
Sod2	0.13
SOD3	8.42
Sqstm1	0.18
Srxn1	0.99
Tpo	8.21
Txn1	3.39
Txnip	0.37
Txnrd1	0.77
Txnrd2	0.73
Txnrd3	2.39
Ucp2	0.28
UCP3	8.41
Vim	0.41
Xpa	1.11
Actb	-0.11
B2m	-0.27
Gapdh	0.32
Gusb	0.19
Hsp90ab1	-0.12
MGDC	6.30

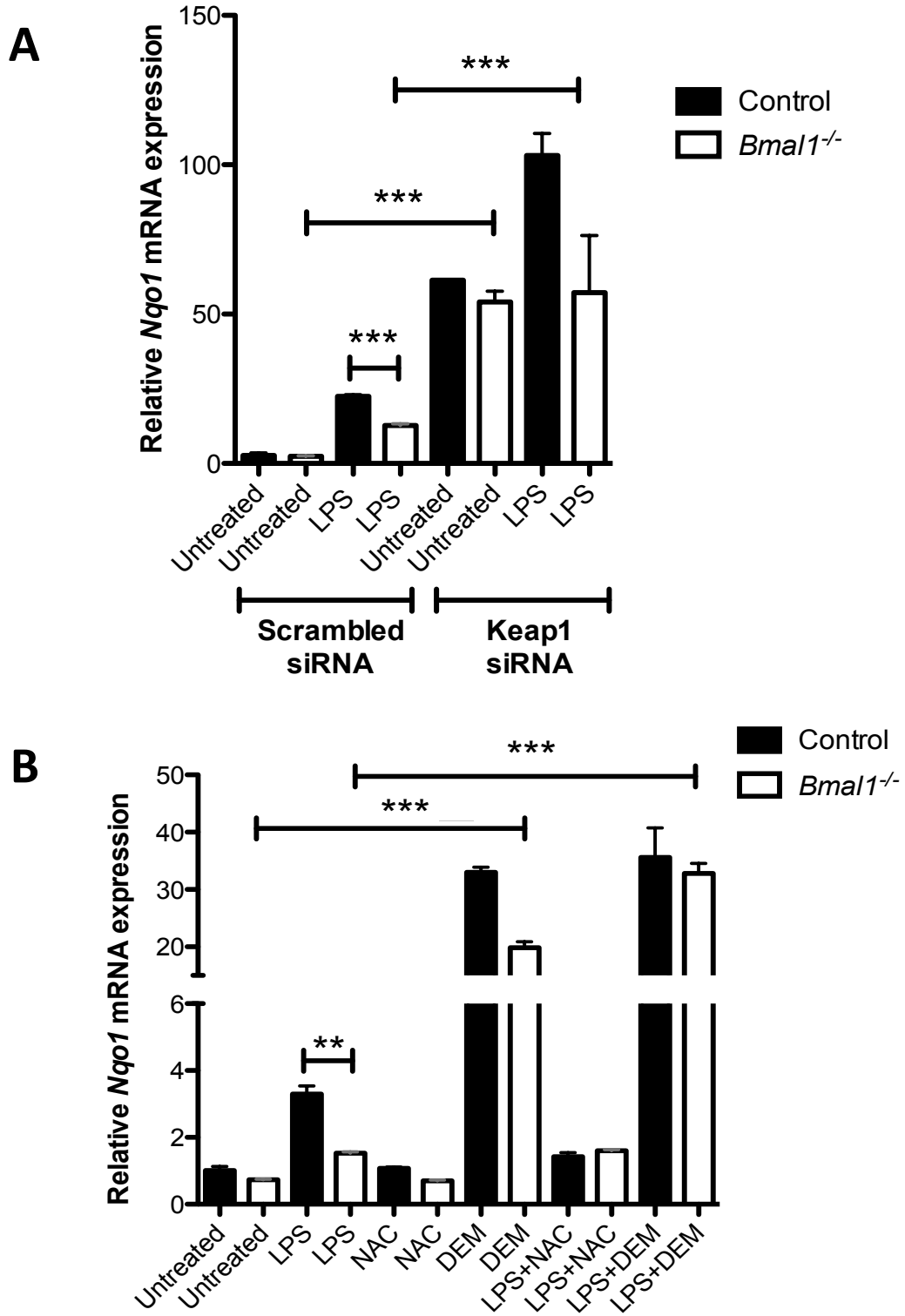
## Supplemental Figure 7



# Supplemental Figure 8



# Supplemental Figure 9



## Supplemental Methods

**Mice.** All mice were maintained according to European Union regulations and the Irish Health Products Regulatory Authority. Experiments were performed under Health Products Regulatory Authority license with approval from the Trinity College Dublin BioResources Ethics Committee. C57BL/6 wild-type mice were bred in house from established colonies. All mice were housed under specific pathogen free conditions and euthanized humanely by carbon dioxide inhalation.

**Generation of bone marrow derived macrophages (BMDMs).** Mice were euthanized in a carbon dioxide chamber and death was confirmed by cervical dislocation. Bone marrow cells were extracted from the leg bones and differentiated in DMEM (containing 10 % foetal calf serum (FCS), 1 % penicillin streptomycin (p/s) and 20 % L929 supernatant) for 6 days. They were then counted and plated for experiments.

**Cell culture.** Peritoneal cells were seeded at  $1 \times 10^6$  cells per well in serum-free media, and after 45 minutes non-adherent cells were washed out and attached cells were harvested immediately for RNA analysis or western blotting. For ROS measurements, cells were stained with CD11b<sup>+</sup> antibody to select specifically for myeloid cells. For synchronization experiments with BMDMs, media containing 50 % horse serum was applied to the cells for two hr to initiate serum shock (1).

**RT-PCR.** Cells were lysed and total RNA was extracted using the RNAeasy kit (Qiagen) and was reverse-transcribed using High-Capacity cDNA Reverse Transcription Kit (Applied Biosystems) according to the manufacturers' instructions. This cDNA served as a template for amplification of target genes by real-time PCR. The cycling threshold method [ $2^{-(\Delta\Delta Ct)}$ ] was used for relative quantification by comparative method after normalization to *Rps18*, an endogenous control gene.

Primers for RT-PCR were generated using Primer Quest on mRNA sequences obtained from the NCBI nucleotide database. The primers were then checked using in silico PCR in UCSC genome browser. It was ensured that primers crossed an exon-exon border with an intron of at least 1000bp where possible. Primer BLAST was used to check primers for specificity to the gene of interest. A 4-point standard curve assay was used to test efficiency of the primers.

### **Primers**

*Il-1b* (F: GGAAGCAGCCCTTCATCTTT, R: TGGCAACTGTTCCCTGAACTC),

*Rps18* (F: GGATGTGAAGGATGGGAAGT, R: CCCTCTATGGGCTCGAATTT).

*Bmal1* (F: TGCAATGTCCAGGAAGTTAGAT, R: GTTTGCTTCTGTGTATGGGTTG),

*Nrf2* (F: CACATCCAGACAGACACCAG, R: ATGGGAATGTCTCTGCCAAA),

*Hmox1* (F: GGAAGCAGCCCTTCATCTTT, R: TGGCAACTGTTCCCTGAACTC),

*Gsr* (F: GGAAGCAGCCCTTCATCTTT, R: TGGCAACTGTTTCCTGAACTC),

*Nqo1* (F: GCTGCAGACCTGGTGATATT, R: TGTAGGCAAATCCTGCTACG).

### **Primers for affinity purification with biotinylated nucleotide (oligo pulldown)**

E-box forward: 5'-(BIO)-GAGCCCAGGGCACGTGGGAGAAGTGG-3'

E-box reverse: 5'-CCACTTCTCCCACGTGCCCTGGGCTC-3'

Scrambled forward: 5'-(BIO)-GAGCCCAGGGATGTTCGGGAGAAGTGG-3'

Scrambled reverse: 5'-CCACTTCTCCTCGCATCCCTGGGCTC-3'

**Western Blotting.** Cells were lysed in SDS sample buffer [0.125 M Tris pH 6.8, 10% (vol/vol) glycerol, 0.02% SDS] and [immunoblot](#) analysis was carried out. [Immunoblots](#) were developed using autoradiographic film or using a ChemiDoc MP gel imaging system (Bio-Rad).

**ELISA.** For detection of IL-6 and TNF $\alpha$  in BMDMs, supernatants were collected and cytokines quantified by ELISA according to manufacturers' instructions (R&D Systems). For detection of IL-1 $\beta$  in mouse serum, serum was isolated from whole blood and IL-1 $\beta$



was quantified by quantikine ELISA (Quantikine, MLB00C). Results [are](#) presented as mean  $\pm$  SEM.

**Reagents.** Reagents used, LPS (*E. coli*, serotype EH100, Alexis); ELISA kit used, IL-6 (Duoset DY406-05), TNF $\alpha$  (Duoset DY410-05), IL-1 $\beta$  (Quantikine, MLB00C). Antibodies used:  $\beta$ -actin (4267), BMAL1 (14020), NRF2 (D1Z9C) KEAP1 (D6B12), (Cell Signaling Technologies), IL-1 $\beta$  (R&D, AF401-NA), HIF-1 $\alpha$  (NB100-449) (Novus). siRNAs used: *Nrf2* (4390771/570522), *Keap1* (4390771/578525), *Bmal1* (4390771/562620), silencer select negative control siRNA (4390843). Lipofectamine RNAiMax (Thermo Fisher Scientific). Flow cytometry and confocal stains used, CellROX (Thermo Fisher Scientific) and MitoTracker green (Thermo Fisher Scientific).

**Transfection.** BMDMs were seeded at  $5 \times 10^5$  cells/well. On the next day, cells were transfected with 10 nM of a given siRNA or a scrambled siRNA negative control using Lipofectamine RNAiMax (Invitrogen) for 24 [hr](#). Media was replaced the following day and experiments were carried out as individually described.

**Glutathione assay.** Free reduced glutathione was determined using the luminescence-based GSH-Glow glutathione assay (Promega), which is based on the conversion of a luminogenic probe in the presence of reduced GSH in a reaction catalyzed by GST. Luminescence measurements were performed in triplicates for each biological replicate and processed in a single run to aid comparative quantification. Relative luminescence units (RLUs) were

corrected for background luminescence and converted to nanomoles per milligram of protein using a standard curve for reduced GSH.

**ROS measurement.** BMDMs were cultured at  $5 \times 10^5$  cells per well. Cells were stained with 5  $\mu$ M CellROX (Invitrogen, US) for 30 minutes at 37 °C. Cells were subsequently stained with Aqua Live/Dead stain for 30 minutes at 37 °C. The cells were washed in PBS and analyzed using a CyAn flow cytometer. The data was analyzed using FlowJo software. The intracellular locus of ROS production was investigated by examining cells stained with CellROX using an epifluorescent live cell-imaging microscope (Zeiss ObserverZ1). ROS production was assessed by dual labeling of cells with CellROX and a mitochondrial-specific probe (Mitotracker Green, Invitrogen). Cells were stained with CellROX (5 mM) and Mitotracker Green (50 nM) for 30 minutes at 37 °C, washed in PBS and then visualized by epifluorescent microscopy at 37 °C. All imaging was performed within 2 hr of staining.

**Graphing of rhythms in peritoneal cells and serum shock.** The data were plotted against time in hours and the presence of circadian patterns was assessed using multiple regression to fit a linearized cosinor model with a pre-determined period of 24 hr (2). Circadian patterns were indicated by statistical significance of the predicted cosinor (sine and cosine) regression coefficients. The cosinor model was defined by linear sine and cosine terms of transformations of the time variable in hours:

$$Y_i = M + \beta \text{Cos} (2\pi t_i / 24) + \gamma \text{Sin} (2\pi t_i / 24)$$

Where Y is time in hours, and M, b and g were predicted by regression (2). The cosinor curve provided a graphical representation of how closely the data approximated to the 24 hr

periodicity of a circadian dataset, and the statistical significance of this was determined by testing the null hypothesis that the amplitude of the curve was equal to zero.

### **ChIP-seq database analysis**

Fastq data for two ChIP-Seq samples from the GEO series GSE95712 (3) were downloaded from NCBI: Bmal1 LPS0h (GSM2522477, 22,927,364 reads) and Input for WT (GSM2522481, 11,237,429reads). The reads were mapped against the mouse assembly mm10 using Bowtie 2 version 2.1.0 with the very-sensitive-local settings, achieving an overall alignment rate of 95% and 98%, respectively. Filtering for mapping quality of at least 30 resulted in BAM files with 16,980,292 and 5,866,323 reads, which were then used for peak calling. This was carried out through GEM (4) under default settings and produced a list of 697 predicted peaks at a false-discovery rate of 0.05. The BAM files were converted into BigWig files and loaded into the UCSC Genome Browser for visualization.

### **References**

1. Balsalobre A, Damiola F, & Schibler U (1998) A serum shock induces circadian gene expression in mammalian tissue culture cells. *Cell* 93(6):929-937.
2. Cornelissen G (2014) Cosinor-based rhythmometry. *Theoretical biology & medical modelling* 11:16.
3. Oishi Y, *et al.* (2017) Bmal1 regulates inflammatory responses in macrophages by modulating enhancer RNA transcription. *Scientific reports* 7(1):7086.
4. Guo Y, Mahony S, & Gifford DK (2012) High resolution genome wide binding event finding and motif discovery reveals transcription factor spatial binding constraints. *PLoS computational biology* 8(8):e1002638.